Interpretation of constant suction direct shear test

Sam Bulolo[1] and *Eng-Choon* Leong[2*]

[1]Kyambogo University, Department of Civil and Environmental Engineering, Uganda
[2]Nanyang Technological University, School of Civil & Environmental Engineering, Singapore

Abstract. Constant suction direct shear test enables the understanding of the failure mechanism in rainfall-induced landslides. It can be conducted using a conventional direct shear apparatus with some modifications. The constant suction direct shear test is carried out in two stages. In the first stage, the unsaturated soil specimen is consolidated to the target net normal stress and matric suction then sheared in the second stage. Matric suction is usually controlled using the axis-translation principle. It is commonly observed that the shear stress of an unsaturated soil sheared in the direct shear shows a strain-hardening behaviour at large displacements making the determination of the failure stress difficult. Hence, the objective of this study is to critically examine the constant suction direct shear tests and the analysis of the test results to obtain the shear strength parameters for unsaturated soils. Constant suction direct shear test data were collated from the literature. It was found that the interpretation of the direct shear test has two inconsistencies: (1) taking failure shear stress at arbitrary displacement strain or limit, dependent on the size of the direct shear apparatus, and (2) correcting only shear stress for contact area. The effect of these two consequences on the interpretation of the direct shear test range from negligible to significant. The study shows that arbitrary determination of failure shear stress can be resolved by plotting the direct shear test results using a stress-path plot. The effects of area correction are shown to be almost negligible for small horizontal displacements of less than 2 mm for both square and circular shear boxes. A more consistent interpretation of the constant suction direct shear test is demonstrated where both these inconsistencies are considered.

1 Introduction

The shear strength of unsaturated soils is one of the key soil parameters in understanding the mechanical behavior of unsaturated soils. Engineering projects such as dams, roads, embankments, etc., involve compacted soils that are unsaturated. The shear strength of unsaturated soils is greatly affected by changes in the matric suction.

Test equipment to determine shear strength parameters for unsaturated soils is usually modified from conventional test equipment for saturated soils [1–4]. Modifications to the conventional triaxial, or direct shear apparatuses to test unsaturated soils is either for suction control or suction measurement during shearing. However, the triaxial test presents many problems such as difficulty in preparing a homogeneous compacted specimen, longer drainage path, and hence, longer testing time. As an alternative, the direct shear test for compacted specimen is attractive as the specimen being thinner is easier to prepare, and the specimen has a much shorter drainage path.

For testing unsaturated soils, several techniques have been used to control suction such as osmotic and vapor equilibration techniques [5–8] and axis-translation technique [9–12]. Regardless of the suction control technique used, testing unsaturated soil requires more tests, longer testing time, and more complicated and expensive equipment as compared to testing saturated soil. Similar to the triaxial test, it is possible to conduct a multistage direct shear test for both saturated and unsaturated soils [13]. If suction needs not to be maintained constant during the shearing, the conventional direct shear box apparatus can be used without modification to obtain a conservative estimate of the shear strength of unsaturated soil [14]. It is, therefore, attractive to investigate further the use of the direct shear box apparatus to obtain reliable unsaturated shear strength parameters for practical application.

During shearing, the volumetric behavior of the soil can be either dilative or compressive. Generally, soils sheared at low constant suction values experience compressive behavior, and the compression increases with an increase in the net normal stress. Dilation is usually observed for soils sheared at higher constant suction values irrespective of the value of the net normal stress. When plotting the peak shear stress with net normal stress, the friction angle of soil can decrease with increasing suction [15, 16], increase with increasing suction [17– 19] or is not affected by matric suction [3, 20]. These observations on the friction angle complicate the interpretation of the shear strength of unsaturated soil and more understanding of the interpretation of the test results is needed.

During a direct shear test, the normal load is kept constant while the shearing area of the specimen reduces. As a result, there is a gradual increase in the normal and shear stresses. Different area corrections have been

* Corresponding author: cecleong@ntu.edu.sg

applied to direct shear test results [21–23]. The direct shear test results are usually reported with either (i) no area correction [24, 25] (ii) area correction applied to both the shear load and the normal load [26, 27], or (iii) area correction applied to only the normal load [28]. These three cases of area correction will be discussed later. The use of area correction to calculate shear stress and normal stress in the direct shear test results increase the accuracy of shear strength determination [21].

The impact of the area correction to interpret constant suction (CS) direct shear test for unsaturated soil is also investigated in this study.

1.1 Shear strength of unsaturated soils.

Research shows that there exists a close relationship between soil-moisture state and shear strength of unsaturated soils [29– 32] It is widely accepted that the shear strength of unsaturated soils can be expressed based on: (i) the effective stress principle or single stress variable, similar to saturated soils [33– 35] and, (ii) the two stress-state variables principle [10, 36]. Equations 1 and 2 are the most widely used shear strength equations for unsaturated soils representing the use of single stress state variable and two stress-state variables, respectively.

$$\tau = c' + \left[(\sigma - u_a) + \chi (u_a - u_w)\right] \tan\phi' \quad (1)$$

$$\tau = c' + (\sigma - u_a)\tan\phi' + (u_a - u_w)\tan\phi^b \quad (2)$$

where τ = shear strength, c' = effective cohesion, σ = total normal stress, u_a = pore-air pressure, u_w= pore-water pressure, χ = coefficient having values ranging between 0 to 1 depending on the degree of saturation, ϕ' = effective friction angle, and ϕ^b = angle indicating a change in shear strength related to matric suction$(u_a - u_w)$. Equation 2 is also known as the extended Mohr-Coulomb criterion (Fredlund et al. 1978). The terms $\chi(u_a - u_w)\tan\phi'$ and $(u_a - u_w)\tan\phi^b$ Equations 1 and 2, respectively, show the shear strength changes arising from changes $(u_a - u_w)$. Experimental results show that there is no unique relationship between χ (used in the single stress state variable framework) and the degree of saturation but rather χ depends on soil type as well as degree of saturation. Therefore, the effect of matric suction on shear strength of soil is non-uniform and non-homogeneous [37. 38]. Research has shown that ϕ^b is not constant and is non-linear over a wide range of suctions [2, 39].

Equations 1 and 2 can be rewritten as Equation 3 where total cohesion C is a combination of effective cohesion and the shear strength contribution from the matric suction.

$$\tau = C + (\sigma - u_a)_f \tan\phi' \quad (3a)$$

where

$$C = c' + \chi (u_a - u_w)_f \tan\phi' \quad (4b)$$

or

$$C = c' + (u_a - u_w)_f \tan\phi^b \quad (3c)$$

Hence by plotting τ versus $(\sigma - u_a)_f$, the y-axis intercept is given by C and the gradient of the line is given by tan ϕ'.

Contradictory observations on the effect of matric suction on friction angle in constant suction (CS) direct shear tests indicate either that void ratio changes with net normal stress and hence the friction angle or matric suction is not constant during the CS direct shear test. Figure 1 illustrates the above observations. Figure 1a shows failure envelopes with different slopes for different suction values [27, 40– 42] while Figure 1b shows failure envelopes with a constant slope for different suction values [4, 43, 44]. It is therefore prudent to understand these inconsistencies in the interpretation of the constant suction direct shear test.

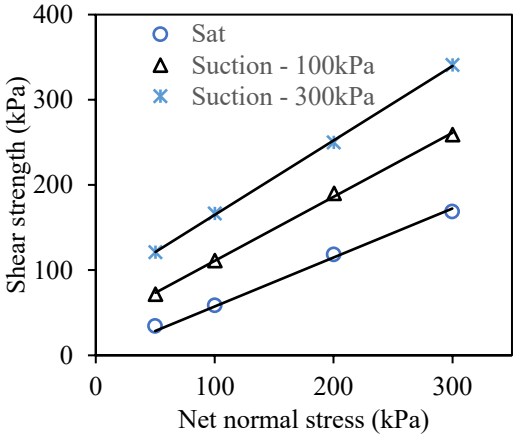

(a) Different slopes (best-fit lines)

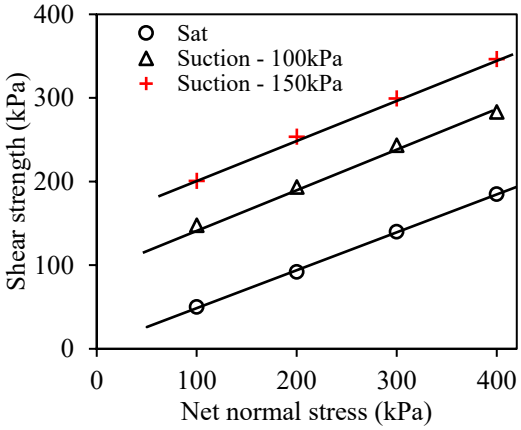

(b) Single slope

Fig. 1. Shear stress versus net normal stress for constant suction direct shear tests.

2 Methodology

Data from the literature on constant suction (CS) direct shear tests were collated for this study. Test results from [4], [40], [42], [45], [47] and [48] were used and the details are summarized in Table 1.

For all the soils in Table 1, the shear test results were re-analysed by (1) correcting the normal and shear stresses for the area, and (2) plotting the stress path using

the uncorrected and corrected normal and shear stresses. unsaturated shear strength parameters from direct shear tests with results reported using different slopes for each matric suction were re-interpreted using a saturated soil slope.

Firstly, the saturated tests were re-interpreted using the stress path for the corrected and uncorrected normal and shear stresses to compare the re-interpreted c′and ϕ′ with the reported c′and ϕ′. Next, the CS direct shear test results were reinterpreted by plotting the stress paths and drawing the failure envelope for each suction using a constant slope of tan ϕ' to determine C.

Table 1. Properties of soils used in this study

Reference / Property	Hossain and Yin (2010)	Gu et al. (2019)	Zhou et al (2016)	Gallage and Uchimura (2016)	Mohamed et al (2006)
Soil type	Silty sand	Silty clay	Silty sand	Edoaki silty sand	Sandy silty clay
Liquid limit, LL (%)	32.8	28.3	38	NP	95
Plasticity index, PI (%)	10.1	11.1	10	NP	50
Gravel (%)	5.8	0	0	0	1.7
Sand (%)	44.1	13	100	83.5	47
Silt (%)	36.8	82	0	14.5	11.3
Clay (%)	13.3	5	0	2	40
D_{50} (mm)	0.06	0.02	0.32	0.22	0.04
D_{60} (mm)	0.14	0.03	0.40	0.28	0.13
Specific gravity, G_s	2.60	2.69	2.68	2.75	2.68
USCS	SM	MH	SM	SM	MH
Coef. of curvature, C_c	0.47	1.19	0.90	3.03	0.004
Coef. of uniformity, C_u	30.00	9.33	4.44	16.47	433.33
Porosity, n	1.256	1.599	1.346	1.444	1.078

3 Results and discussion

The three cases of area correction are discussed here. For no area correction, in case (i), the stress path is a vertical straight line (OA) while case (ii) area correction for both shear and normal load and case (iii) area correction for normal load only give a stress path that curves to the right as illustrated by OA′ in Figure 2. For cases (ii) and (iii), soils that clearly show a peak shear stress will show the stress path following line OA′C with the peak as a point on the failure line AB. The area correction is negligible for small horizontal displacements of less than 2 mm for both the square and circular shear boxes.

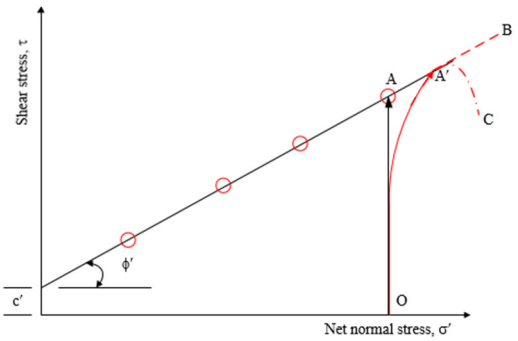

Fig. 2. Stress paths from a saturated direct shear test.

The stress path approach was used to first determine the effective stress shear strength parameters, c′ and ϕ′. A typical illustration of the use of the stress path approach for the interpretation of the saturated tests from Han [48] is shown in Figure 3.

Figure 3a shows that the corrected shear stress versus horizontal displacement plot shows a lower maximum shear stress. However, when the corrected shear and normal stresses during the test were plotted as a stress path, the stresses eventually falls on the same failure line as illustrated in Figure 3b.

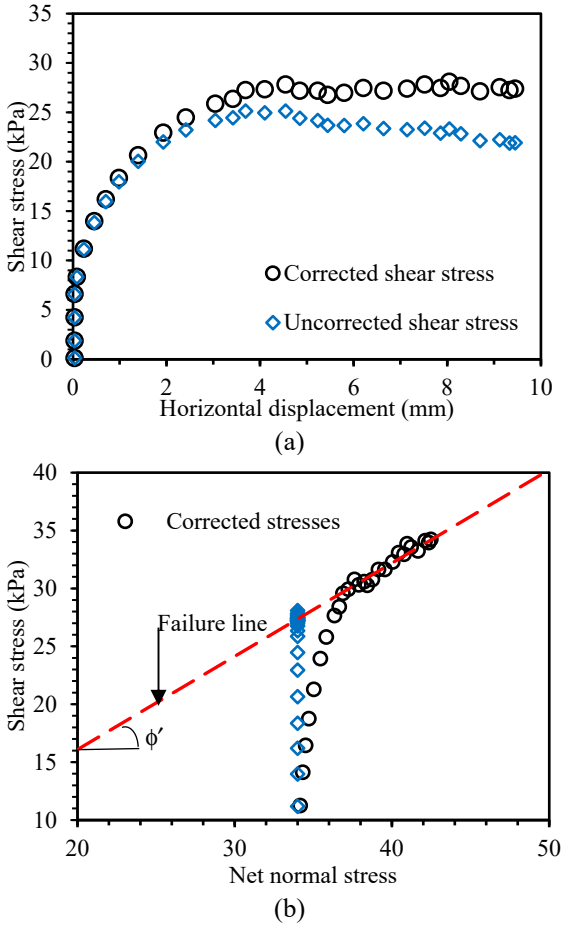

Fig. 3. Illustration of the use of stress path to interpret constant suction direct shear tests from Han [48] with no peak shear stress.

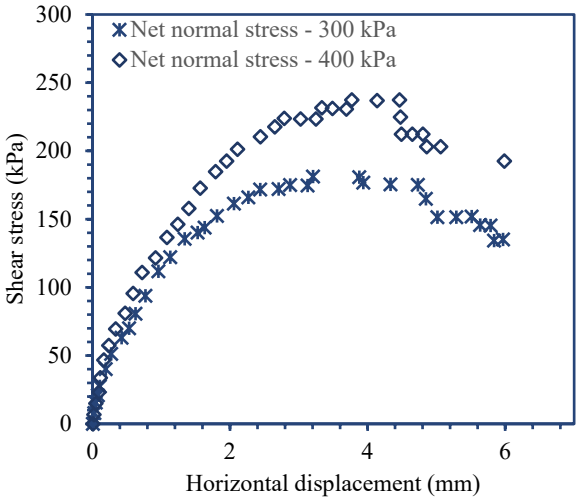

(a) Shear stress versus horizontal displacement

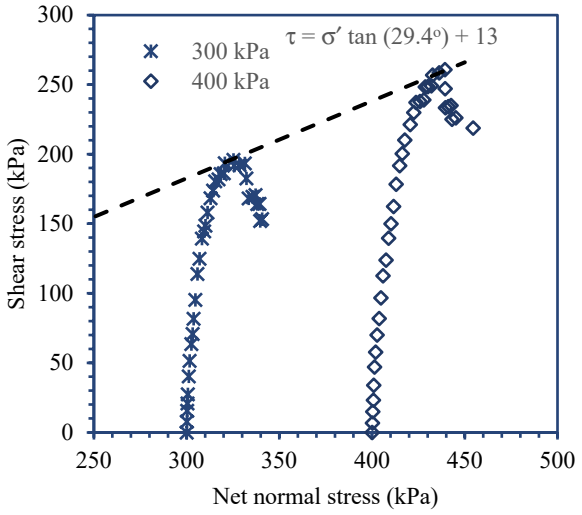

(b) Stress paths

Fig. 4. Shear stress versus horizontal displacement and stress paths for constant suction direct shear tests from Han [48] with peak shear stress.

Figure 4(a) shows an example of direct shear test results from Han [48] showing strain-softening behavior for both uncorrected and corrected shear stresses. Figure 4(b) shows the stress paths for both uncorrected and corrected stresses. The c′ and ϕ′ obtained from the stress paths using corrected stresses in Figure 4(b) are 16 kPa and 29.1°, respectively, as compared with the reported values of 13 kPa and 29.4°, respectively. Hence, the use of corrected stresses in the stress path affects the value of c′ more than the value of ϕ′ for soil showing strain-softening behavior in the direct shear test.

Figure 5 shows a plot of the corrected shear stress versus the corrected net normal stress for the CS direct shear test conducted at a suction of 50 kPa. Using the effective shear strength slope (thick line), each net normal stress indicates a different C. Zhang [49] showed that the matric suction of unsaturated soils sheared under constant matric suction cannot be controlled precisely and this may have affected the quality of the test results in CS tests and hence the interpretation of the CS direct shear test. A Conservative estimate of C for each suction can be obtained using the stress path at the lowest net normal stress. Using such an approach C can be similarly obtained from tests conducted at other constant suctions. By plotting, C versus suction, c′ can be obtained from the y-intercept at suction of 0 kPa. Figure 6 shows a plot of C versus suction for four different soils.

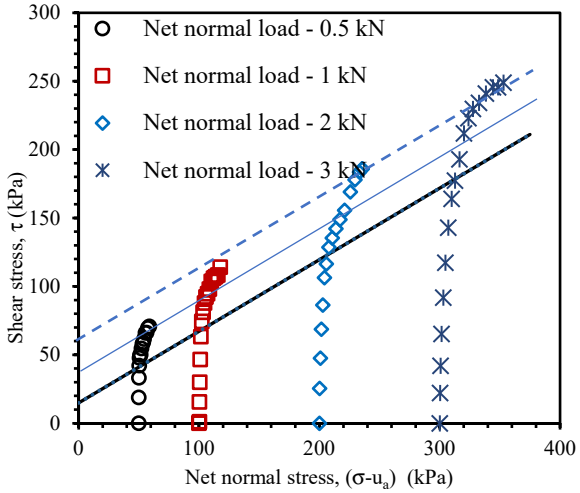

Fig. 5. Stress paths for unsaturated direct shear tests for CDG at 50 kPa matric suction (data from Hossain and Yin [19]).

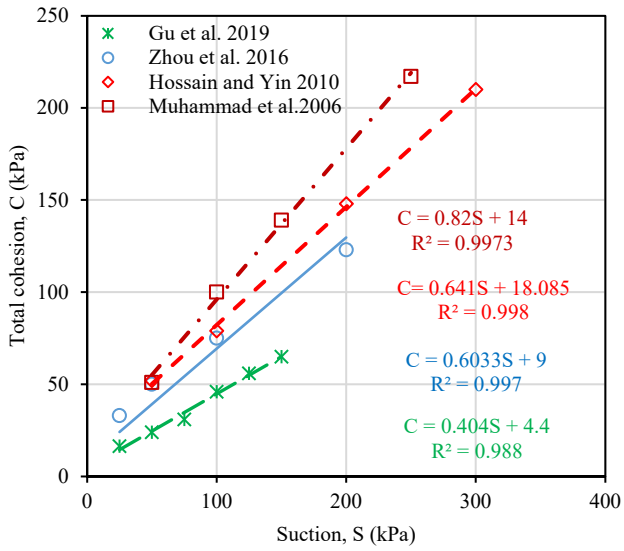

Fig. 6. Re-interpreted data for case of different slopes.

Figure 7 compares the reported c′ and ϕ′ with the same parameters obtained from the stress path approach. It can be seen that there is almost a one to one correspondence. This means that the saturated test can be minimised or even eliminated since c′ and ϕ′ can be recovered from the CS direct shear tests using the stress path approach described here.

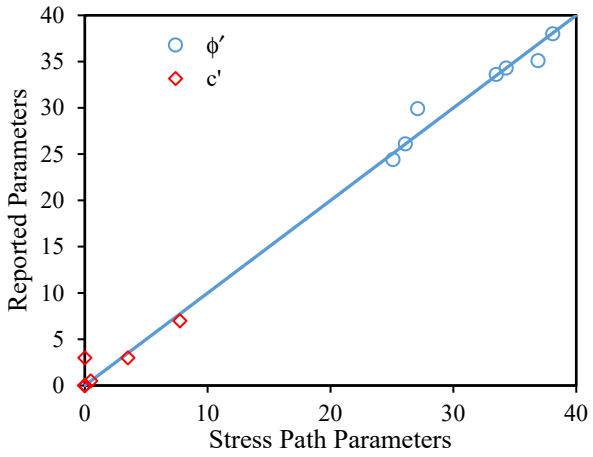

Fig. 7. Reported versus stress path effective cohesion and effective friction angle

4 Conclusion

It has been demonstrated that for a CS direct shear test, the area correction can help to better interpret the test results. The failure point should be on a failure line where the slope is given by the tangent of the effective friction angle. Using the corrected shear and normal stresses, the stress path can be plotted for each test at a constant suction. For strain-softening tests, the failure points will all lie on the failure line with slope given by the tangent of the effective friction angle. For a strain-hardening test, the stress path eventually follows the failure line. From a series of CS direct shear tests at different constant suction values, the effective cohesion c' can be recovered from the y-intercept of a plot of total cohesion C versus suction.

References

1. F. Melinda, H. Rahardjo, K. K. Han, and E. C. Leong, *J. Geotech. Geoenvironmental Eng.*, **130**, 8, 807–817, (2004)
2. V. Escario and J. Saez, *Geotechnique*, **36**, 3, 453–456, (1986)
3. R. Schnellmann, H. Rahardjo, and H. R. Schneider, *Eng. Geol.*, **162**, 88–96, (2013)
4. T. Gu, J. Wang, C. Wang, Y. Bi, Q. Guo, and Y. Liu, *J. Soils Sediments*, **19**, 10, 3463–3475, (2019)
5. J. Blatz and J. Graham, *Geotechnique*, **50**, 4, 465–469, (2000)
6. P. Delage and Y. J. Cui, *Geomech. Geoengin.*, **3**, 1, 1–11, (2008)
7. J. A. Blatz, Y.-J. Cui, and L. Oldecop, *Geotech. Geol. Eng.*, **26**, 6, 661–673, (2008).
8. A. Hamidi, G. Habibagahi, and M. Ajdari, *Geotech. Test. J.*, **36**, 1, (2013)
9. J. Hilf, (1956).
10. D. G. Fredlund and N. R. Morgenstern, *J. Geotech. Div.*, **103**, GT5, 447–466, (1977)
11. C. W. W. Ng, Y. Cui, R. Chen, and P. Delage, *Soils Found.*, **47**, 4, 675–684, (2007)
12. S. Tripathy, H. Elgabu, and H. R. Thomas, *Geotech. Test. J.*, **35**, 1, 91–102, (2012)
13. S. Nam, M. Gutierrez, P. Diplas, and J. Petrie, *Eng. Geol.*, **122**, 3–4, 272–280, (2011)
14. A. Tarantino and G. El Mountassir, *Eng. Geol.*, **165**, 89–104, (2013)
15. P. Delage, G. P. R. Suraj de Dilva, and E. Laure, in *International Journal of Rock Mechanics and Mining Sciences & Geomechanics Abstracts*, 1988, **25**, 3, 114.
16. A. Maatouk, S. Leroueil, and P. LA Rochelle, *Géotechnique*, **45**, 3, 465–477, (1995).
17. E. Cokca, O. Erol, and F. Armangil, *Geotech. Geol. Eng.*, **22**, 2, 285–297, (2004)
18. V. Merchan, J. Vaunat, E. Romero, and T. Meca, in *1st European conference on unsaturated soils*, 2008, 423–428.
19. A. Hossain and J. Yin, *Can. Geotech. J.*, **47**, 1112–1126, (2010)
20. W. Ye, Y. Zhang, B. Chen, X. Zhou, and Q. Xie, *J. Rock Mech. Geotech. Eng.*, **2**, 2, 155–161, (2010)
21. Š. Skuodis and T. Tamosiūnas, *Sci. - Futur. Lith.*, **6**, 5, 499–503, (2014) [Online]. Available: http://www.mla.vgtu.lt/index.php/mla/article/view/mla.2014.71
22. J. Lai, (2004).
23. Y. Dong, Y. C. Wang, L. G. Lu, and W. Wang, *Appl. Mech. Mater.*, **405–408**, 353–357, (2013)
24. ASTM D3080/D3080M-11, *ASTM International, West Conshocken, PA, 2012*. West Conshohocken, PA, 2012, 1–9, 2012.
25. BS EN ISO 17892-10, 2018.
26. C. Gallage and T. Uchimura, *J. Geotech. Geoenvironmental Eng.*, **142**, 3, 1–9, (2016).
27. B. J. Shwan and C. C. Smith, in *ICE Proceedings of the XVI ECSMGE Geotechnical Engineering for Infrastructure and Development*, 2015, ISBN 978-0-7277-6067-8, 3353–3357.
28. V. N. . Murthy, in *Geotechnical Engineering: Principles and Practices of soil Mechanics and Foundation Engineering*, 1st ed., M. . Bowers and B. . Broms, Eds. CRC Press, 2002, 287–288.
29. J. E. B. Jennings and J. B. Burland, *Géotechnique*, **12**, 2, 125–144, (1962)
30. D. G. Fredlund, N. R. Morgenstern, and R. A. Widger, *Can. Geotech. J.*, **15**, 3, 313–321, (1978)
31. S. K. Vanapalli, D. E. Pufahl, and D. G. Fredlund, *Proc. 51st Can. Geotech. Conf.*, 87–94, (1998).
32. Y. Matsushi and Y. Matsukura, *Bull. Eng. Geol. Environ.*, **65**, 4, 449–455, (2006)
33. D. Croney, J. Coleman, and W. Black, (1958).
34. A. W. Bishop and G. E. Blight, *Géotechnique*, **13**, 3, 177–197, (1963)
35. A. Bishop, *Tek. Ukebl.*, **39**, 859–863, (1959).
36. D. G. Fredlund, H. Rahardjo, and M. D. Fredlund, *Unsaturated Soil Mechanics in Engineering Practice*. 2012.
37. E. C. Leong, in *Indian Geotechnical Conference*, 2016, **103**, 5, 447–466.

38. N. Lu and W. J. Likos, *J. Geotech. Geoenvironmental Eng.*, **132**, 2, 131–142, (2006)
39. J. K. Gan and D. . Fredlund, Hong Kong, (1992).
40. M. A. Hossain and J. H. Yin, *J. Geotech. Geoenvironmental Eng.*, **136**, 1, 189–198, (2010)
41. W. J. Likos, A. Wayllace, J. Godt, and N. Lu, *Geotech. Test. J.*, **33**, 4, (2010).
42. T. A. Mohamed, F. H. Ali, S. Hashim, and B. B. K. Huat, *Am. J. Environ. Sci.*, **2**, 4, 142–145, (2006)
43. W. H. Zhou, X. Xu, and A. Garg, *Meas. J. Int. Meas. Confed.*, **93**, 351–358, (2016)
44. S. Sun and H. Xu, in *Schanz T . (eds) Experimental Unsaturated Soil Mechanics. Springer Proceedings in Physics, Springer, Berlin, Heidelberg*, **112**, 2007, 195–206.
45. A. Zhou and D. Sheng, *E3S Web Conf.*, **9**, January, 974–987, (2016)
46. C. P. K. Gallage and T. Uchimura, *Soils Found.*, **50**, 1, 161–172, (2010)
47. C. Gallage and T. Uchimura, *J. Geotech. Geoenvironmental Eng.*, **142**, 3, 2017, (2016)
48. K. K. Han, Nanyang Technological University, Singapore, 1997.
49. X. Zhang, in *International Journal for Numerical and Analytical Methods in Geomechanics*, 2015, **40**, June 2015, 269–296.